Transportation Infrastructure Geotechnology (2026) 13:24
https://doi.org/10.1007/s40515-025-00777-4

RESEARCH

Effect of TBM Disc-Cutter Wear on Granite Rock Fragmentation for Kani Sib Water-Conveyance Tunnel Project

Mansour Sabri[1] · Ebrahim Sharifi Teshnizi[2] · Kamran Goshtasbi[1] · Hamid Reza Nejati[1] · Ehsan Taheri[1] · Brendan C. O'Kelly[3]

Received: 29 September 2025 / Accepted: 17 December 2025

Abstract
This case-study research article investigates the effects of normal abrasive wear to the disc cutters located in the tunnel-boring machine's (TBM's) cutter-head used for excavating through the highly abrasive granite/granodiorite rock mass at the northeast section of the Kani Sib Water-Conveyance Tunnel (KSWCT) project, Iran. The Rock Failure Process Analysis method was employed to investigate the impact of wear (0–20 mm abrasion depth) to single- and double-disc cutters on the rock fragmentation process, integrating Weibull-distributed heterogeneity to the behaviour model. Validated against Brazilian tensile strength test results, the numerical simulations reveal that progressive wear of the cutter blades causes the failure mode for the KSWCT granite rock to transition from efficient brittle fracture (sharp cutters) to energy-intensive ductile-type failure (worn cutters), thereby increasing the peak indentation (cutting) force requirement by 20–40%. Stress distribution analysis demonstrates a sharp concentrated stress profile observed ahead of new disc cutters indenting into intact granite rock, whereas the worn cutters generate diffuse stress fields, delaying rock fragmentation. A 12 mm cutter-wear threshold (beyond which the energy consumption for crack propagation increased by 35%) was identified to mitigate efficiency losses for tunnelling in the KSWCT granite rock, thereby providing a data-driven basis for predictive cutter-disc maintenance in mechanised tunnelling operations.

Keywords Rock cutting · Disc-cutter wear · Rock failure process

Extended author information available on the last page of the article

Published online: 27 January 2026

1 Introduction

Mechanised tunnel excavation commonly employs tunnel boring machines (TBMs). Centrally important to the TBM excavation efficiency is the cutting process of the disc cutters mounted in the TBM's cutter-head. This aspect has been widely researched, primarily using indentation tests, but also numerical modelling approaches. For instance, Chen and Labuz (2006) employed a wedge-shaped indentation tool, along with monitoring of acoustic emission parameters, to investigate the influence on rock fracture of (i) the cutting tool geometry, (ii) the rock mechanical properties and (iii) the lateral confinement stress. Also using an indentation test and acoustic emission monitoring approach, Ma et al. (2011) studied the effect of the confinement stress on the fragmentation of granite and marble samples caused by a disc cutter. While the force required for crack growth in the granite sample was found to increase with increasing confinement stress, they reported that the required cutting force decreased with increasing confinement stress for the marble sample above a critical confining stress value. Liu et al. (2016) performed sequential indentation tests using disc cutters on granite and sandstone samples to investigate the effect of the confinement stress. They found that there was increased energy consumption with an increase in the minimum lateral stress. Specific energy (SE) — the energy required to excavate a unit volume of rock — is an important parameter for describing the rock excavation efficiency; i.e., reduced SE indicating greater TBM cutting efficiency. Lin et al. (2018) investigated the effect of jointing on concrete samples for double-disc cutters. Their results showed that the SE decreased for larger spacing between the cutters, with 60° joint orientation the most efficient mode in terms of SE. Chen and Song (2018) examined the effect of the bilateral stress on rock fragmentation using an indentation test employing a disc cutter on a granite rock sample. While Wang et al. (2019) performed indentation tests using various disc cutters to determine the optimal penetration depth. They found that in order to reduce the SE of excavation, the penetration depth (d) increases for greater spacing between the cutters.

Additionally, numerical investigations have been performed to examine the rock cutting process achieved using disc cutters. For instance, using numerical modelling based on the two-dimensional (2D) Rock Failure Process Analysis (RFPA) method, Ma et al. (2011) studied the effect of confinement stress on the rock fragmentation achieved using disc cutters. According to their results, the confining stress has a significant effect on the chipping force, crack angle and effective crack length. Wang et al. (2011) employed the 2D RFPA method to investigate the rock fragmentation occurring during tool indentation under static and dynamic loads. Simulation results for the static case showed that brittle rock fragmentation proceeds in a progressive manner during indentation. Whereas the numerical models for the dynamic case depicted radial cracks, incipient chips, pulverised zones and shell cracks. In other words, dynamic loading produced more efficient rock fragmentation than static loading. Other similar numerical studies (Huang et al. 2013; Moon and Oh 2012; Wu et al. 2019; Xu et al. 2021) have investigated the rock fragmentation process for idealised tool–rock interactions, e.g., examining the effect of different spacing between the disc cutters. Numerical models developed by Sabri et al. (2023, 2024) showed that progressive wear of the disc-cutter blade significantly increased the cutting force

— particularly side force — and accelerated the degradation of the cutter's bearing (on account of excessive pressure acting on the cutters due to the geological conditions, disc cutter health and installation radius). It is important to note that during its operational lifetime, the normal abrasive wear to the disc cutter changes the rock–cutter contact profile and interaction area, thereby effecting the required cutting force and also the stress distribution profile within the rock mass.

The present case study concerns the 35.7-km-long Kani Sib Water-Conveyance Tunnel (KSWCT) project — a critical component of Iran's infrastructure, and one of the longest mechanised tunnels in the country. At its northeast end, a 20.3-km long section of the tunnel was excavated through the highly abrasive granite/granodiorite rock mass using a double-shield hard rock TBM plant; its cutter-head fitted with 17-inch (431.8 mm) dia. disc cutters, typical of TBM disc-cutter diameters used elsewhere in the world. The extreme hardness and abrasiveness of the granite/granodiorite rock posed significant challenges, particularly in terms of disc cutter wear, making this section of the KSWCT a focal point for analysing the cutter performance and failure mechanisms. The interplay between the disc cutter wear and the stress distribution and fracture mechanics of the rock directly dictates the TBM's performance. Specifically, this paper presents a numerical investigation of the effect of normal wear to 17-inch (431.8 mm) dia. single- and double-disc cutters on (i) the cutting force for the granite rock, (ii) the resulting changes in the stress regime within the rock mass and (iii) the process of crack initiation and expansion for the granite rock. This article demonstrates the altered interaction dynamics between the disc cutter blade and the granite rock material in response to increasing levels of wear to the blades. It will be demonstrated that new (sharp) cutter blades generate concentrated stresses within the rock, promoting rapid crack initiation and coalescence (brittle failure), whereas the rock indentation force–depth curves produced for worn cutter blades exhibit a more ductile-type behaviour, albeit requiring significantly higher indentation force to induce fracture, such that the TBM's drilling efficiency progressively declines as the disc-cutter wear intensifies.

This case study advances the understanding of disc-cutter wear dynamics through several original contributions. Firstly, it systematically quantifies the impact of blade wear for both single- and double-disc cutters by evaluating six discrete levels of wear intensity (in the range of 0 to 20 mm), a granularity absent in prior studies that often treat wear as a binary or coarse variable. By correlating the wear magnitude with the cutting force escalation, stress redistribution and energy consumption, the present work provides unprecedented resolution into how progressive wear degrades the cutting efficiency — a critical insight for predictive maintenance in tunnelling projects. Secondly, the study uniquely identifies a brittle-to-ductile type transition in the rock failure mechanism in response to the amount of disc-cutter wear. Sharp cutters produce localised stress concentrations and compact indentation force–depth curves that are characteristic of brittle-type fracture in the rock, whereas worn cutters generate diffuse stress fields and elongated indentation force–depth curves that are indicative of more ductile-type rock behaviour. This transition in the rock failure behaviour for sharp and worn disc cutters is rigorously demonstrated for the granite rock samples through principal stress profiles and crack pattern analyses, offering a mechanistic explanation for the wear-driven efficiency losses that prior studies only inferred qualitatively. Thirdly, the comparative analysis of single-disc versus double-disc cutter configurations for different levels of wear introduces nuanced insights into TBM cutter-head design. While the single-disc cutter exhibits asymmetric crack propagation in the granite rock samples, the double-disc cutter leverages inter-disc interactions to mitigate the stress dispersion, thereby enhancing the chip formation efficiency. These findings underscore the importance of the geometric configuration of the disc-cutters located in the TBM cutter-head for wear management, a dimension underexplored in the existing literature. Finally, the study translates numerical findings into a predictive maintenance framework, emphasising wear-level thresholds that trigger efficiency losses. By linking microscale stress patterns (e.g., peak principal stress zones) to macroscale outcomes (e.g., TBM torque demands), this case study offers a holistic strategy for minimising TBM downtime and energy costs — a pragmatic advancement beyond theoretical models. A key methodological innovation lies in the integration of Weibull distributions to model the mesoscale heterogeneity of the granite rock's properties (e.g., elastic modulus, tensile strength). While stochastic material models are not new, their application here in investigating the effect of disc-cutter wear captures the stochastic nature of crack initiation and propagation in the granite rock, offering a more realistic representation of the rock's fragmentation compared to conventional homogeneous models. As such, the investigative approach employed in the present case study bridges the gap between idealised simulations and the real-world geological variability. Collectively, the mentioned innovations establish a new benchmark for integrating stochastic material science, cutter-wear dynamics and operational engineering in TBM research.

2 Case Study: Kani Sib Water-Conveyance Tunnel (KSWCT)

The present case study considers part of the KSWCT project, which transfers water from the Kani Sib Dam to Lake Urmia (located in West Azerbaijan Province, Iran), in order to help with its revival. The tunnel was excavated using a double-shield hard rock TBM plant (6.32-m excavation diameter) manufactured by the NFM-NHI group, with the 20.3-km long section at the tunnel's northeast-end excavated through highly abrasive granite/granodiorite rock formations (Figs. 1 and 2).

Some typical physical and mechanical properties, measured as part of the present investigation for representative granite rock samples sourced from the KSWCT project, are listed in Table 1. In particular, uniaxial compression tests were performed to determine the elastic modulus, Poisson's ratio and unconfined compressive strength (UCS) properties, while triaxial-compression testing was performed to obtain the value of the friction angle parameter.

For the KSWCT project, the TBM cutter-head employed for the granite/granodiorite excavation was equipped with 47 disc-cutter rings (constant cross-section type, each of 17-inch dia.) that were strategically arranged as 8 central cutters, 25 face cutters and 14 radius cutters (Fig. 3). The extreme hardness and abrasiveness of the granite/granodiorite rock posed significant challenges, particularly in terms of disc cutter wear; e.g., over four years of tunnelling works through this rock mass, some 3944 disc-cutter rings required replacement due to their wear and bearing failure.

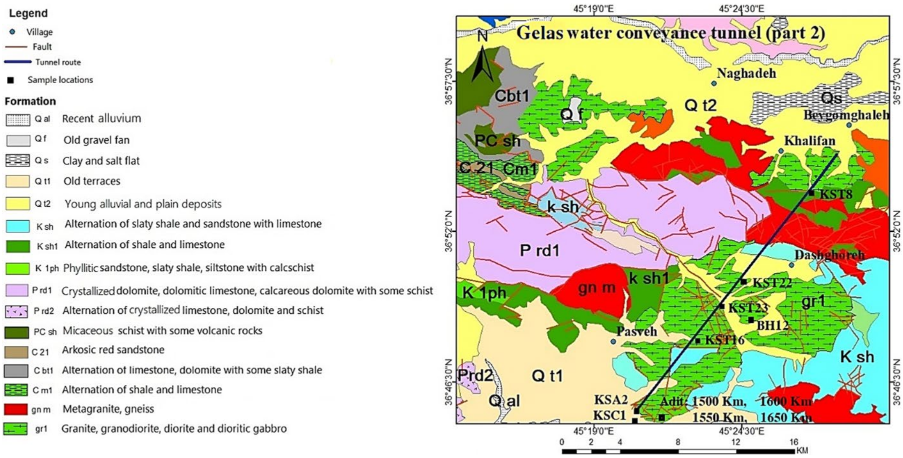

Fig. 1 Geological map of the study area for the KSWCT project

Along with normal wear, the dominant failure modes, as identified Sabri et al. (2023, 2024), included crushing of the cutter's bearing (35%), as well as fracturing, chipping, mushrooming and cracking of the disc cutters themselves (see Fig. 4).

Of the central, face and radius type disc-cutters located on the TBM cutter-head, the central cutters proved the most vulnerable. Some 74% of the failures occurring in central cutters were attributed to crushing of the cutter bearings, caused by elevated lateral forces arising from the asymmetric stress distribution developed during the rock cutting process, and which is exacerbated by their central positioning and concentrated load-bearing role. While less failure-prone than central ones, 44% of the failures in radius disc-cutters occurred due to bearing-type failure, influenced by their installation angle relative to the tunnel curvature, which amplified stress concentrations. Whereas the face disc-cutters demonstrated greater durability, with only a 26% failure rate owing to their alignment that minimised lateral force exposure. Operational impacts over the four years of tunnelling works were quantified through 94 documented cases, where measurable improvements were achieved for replacing > 10% of the disc cutters under stable geological conditions. For instance, the replacement of 17 worn disc-cutters for a 29-m long excavation segment reduced the normal and rolling cutter forces, while enhancing their penetration rates, thereby restoring the TBM's cutting efficiency.

Figure 5 illustrates the changes in the cross-sectional profile measured for a typical 17-inch (431.8 mm) dia. single-disc cutter due to its normal wear in the range of $w = 0$–20 mm. The normal wear pattern of the disc cutter causes the rock–cutter contact area to progressively increase, thereby increasing the required cutting force.

As mentioned in the Introduction, one of the central aims of the present research is to bridge TBM field data and numerical insights of the disc cutter–rock failure mechanisms, emphasising the interplay between the cutter-blade geometry, exerted lateral forces and the blade wear patterns for excavation in abrasive granite/granodiorite rock. As evident from the above discussion, key practical implications include prioritising the replacement of worn central and radius disc-cutters to mitigate TBM

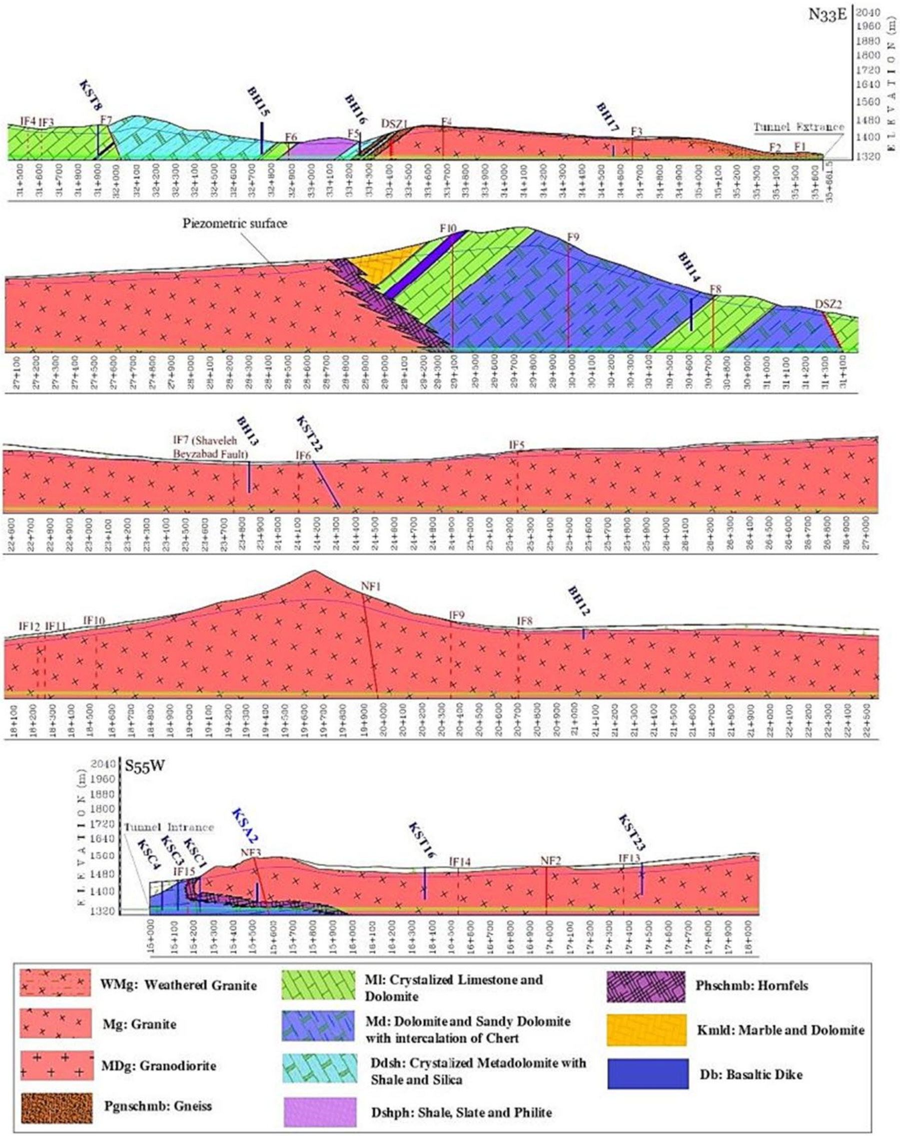

Fig. 2 Cross-section showing the engineering geology along the study area of the KSWCT project

downtime. By demonstrating that proactive cutter management enhances tunnelling advance rates and reduces operational costs, this case study offers actionable strategies for hard rock TBM excavation projects globally. Moreover, the integration of real-world performance metrics with predictive modelling establishes a robust framework for sustaining efficiency in high abrasion rock environments, ensuring that the presented KSWCT case study serves as a benchmark for future tunnelling endeavours.

Table 1 Physical and mechanical properties of representative granite rock samples from the KSWCT project

Parameter	Value
Porosity (%)	0.81
Dry density (kg/m^3)	2700
Saturated density (kg/m^3)	2780
Uniaxial compressive strength, σ_c (MPa)	90–120
Elastic modulus, E_0 (GPa)	35–47
Poisson's ratio, v_0	0.25
Friction angle, φ (degree)	35.2–42.9
Brazilian tensile strength, σ_t (MPa)	7.4–8.0

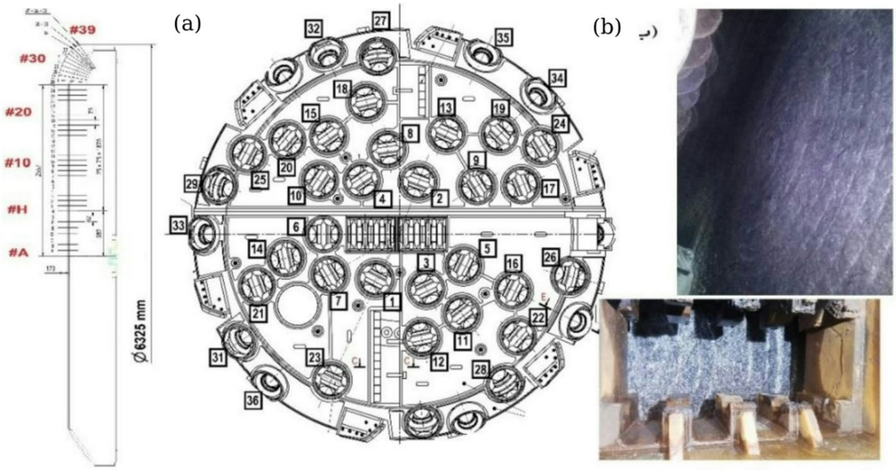

Fig. 3 Double-shield TBM plant (model NTU062) used in the excavation of the northeast section of the KSWCT: (**a**) cutter-head scheme; (**b**) disc trajectories evident on the tunnel face (Sabri et al. 2024)

3 Numerical Simulation Studies

The present investigation employs 2D RFPA models to simulate the rock fracture process caused by single- and double-disc cutters monotonically penetrating into granite rock samples. For more information about the 2D RFPA method and software, the reader is referred to the papers by Tang and Tang (2011, 2020) and Zhu and Tang (2006). Given the widespread adoption of quasi-static 2D numerical analyses by earlier researchers working on this topic — as sumarised in the Introduction section — the quasi-static 2D modelling approach of the present investigation offers a computationally efficient framework for investigating the disc cutter–rock interactions. The quasi-static loading condition is reasonable for slow, steady processes like TBM cutting, but may overlook impact-driven phenomena. Moreover, while inherently simplifying reality (e.g., ignoring the three-dimensional (3D) geometry and dynamic loading effects of the problem, as well as assuming idealised rock behaviour), nevertheless, the 2D model does incorporate advanced statistical methods to enhance realism. For instance, the rock samples were assumed to be composed of large numbers of mesoscopic elements, whose heterogeneous material properties

Fig. 4 Examples of disc-cutter failure patterns for the KSWCT project (Sabri et al. 2023)

were specified using a Weibull distribution (i.e., heterogeneous rock properties were probabilistically assigned across the simulation domain), thereby better approximating the natural granite rock's behaviour. By integrating the Weibull distribution, the model captures the stochastic nature of the granite rock's strength and stiffness, enabling a more nuanced representation of the localised fracture initiation and stress redistribution. Nevertheless, the presented results of the RFPA simulations remain confined to the 2D condition, trading 3D effects (e.g., out-of-plane stress gradients, asymmetric cutter wear) and dynamic phenomena (e.g., inertia, vibrations, transient forces) for computational tractability. Despite these limitations, the combination of statistical heterogeneity modelling with 2D quasi-static mechanics does provide a pragmatic balance, offering actionable insights into the disc cutters' performance and the resulting stress (re-)distribution induced within the rock samples, while aligning with empirical validation practices. As such, the adopted analysis approach is satisfactory for preliminary studies, and particularly sufficient for scenarios where the dominant failure mechanisms are governed by planar quasi-static interactions, provided its assumptions are carefully validated against experimental or field data.

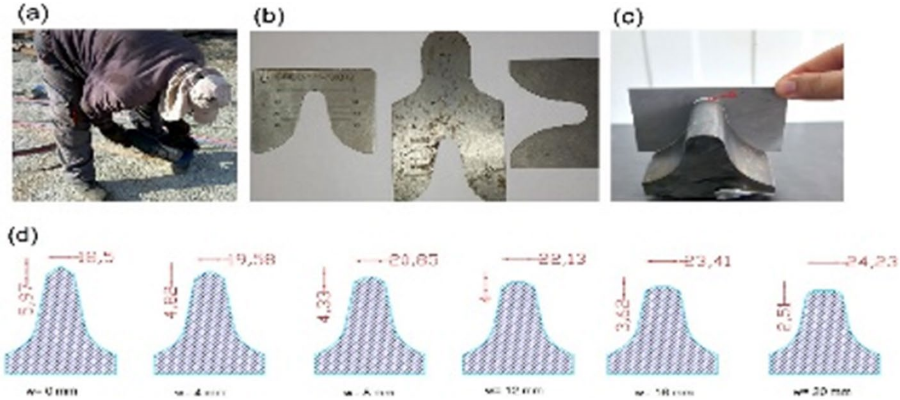

Fig. 5 Determination of the cross-sectional profile changes for normal wear of a single disc cutter: (**a**) sawing off a short section of the disc; (**b**) abrasion measurement tools; (**c**) measuring the amount of cutter wear; (**d**) measured disc cutter cross-sectional profiles for increasing wear amounts in the range of w=0–20 mm (Sabri et al. 2024)

Using the maximum tensile strain and Mohr–Coulomb criterion, elastic damage mechanics was used to describe the constitutive law of the mesoscale elements for the rock samples (Zhu and Tang 2004). In the RFPA method, solids and structures are composed of many mesoscopic same-sized elements, with their mechanical properties given by the following probability density function (Tang and Tang 2011):

$$f_{(u)} = \frac{m}{u_0}\left(\frac{u}{u_0}\right)^{m-1} exp\left[-(\frac{u}{u_0})^{m}\right] \tag{1}$$

where u is the mechanical parameter (elastic modulus, strength, etc.) of the element, u_0 is a scale parameter related to the average of the element parameters, and m is the homogeneity index that defines the shape of the distribution function (note that $m > 1$, with larger m implying more heterogeneous material).

3.1 Model Validation

The 2D RFPA model was validated using the results of the Brazilian tensile strength (BTS) tests performed on representative 54-mm dia. granite rock cores sourced from the KSWCT project. Using the 0.5-mm element size, the rock core in the 2D RFPA model of the BTS test was discretised into a 108 × 108 mesh (11664 elements), adopted to achieve a balance between computational accuracy and practical efficiency. The choice of the 0.5-mm element size was validated through prior studies and mesh sensitivity analyses performed by the 2D RFPA software developers, which confirmed that results stabilise at this mesh density. Moreover, the Weibull-distributed heterogeneous material properties (elastic modulus, strength, etc.) are statistically resolved at this scale, aligning with the mesoscopic heterogeneity of the granite rock material itself.

The inputted mechanical properties for simulating the granite rock core were: (i) a mean BTS of $\sigma_t = 7.7$ MPa; (ii) a mean UCS of $\sigma_0 = 105$ MPa, elastic modulus of $E_0 = 41$ GPa and Poisson's ratio of $v_0 = 0.25$; (iii) a mean frictional angle of $\varphi = 39.0°$; (iv) a homogeneity index of $m = 5$. The steel loading platens of the BTS apparatus were assigned a compressive strength of $\sigma_p = 800$ MPa and an elastic modulus of $E_p = 210$ GPa. Similar to the BTS test that imposed a relative vertical motion of its top loading platen, the RFPA simulation investigated the plane-strain compression of the rock core by applying an external vertical displacement at a constant rate of 0.005 mm/step (i.e., quasi-static loading condition). At each load step, the stress states in some elements comprising the rock core may satisfy the strength criterion (indicating that these elements are damaged), in which case they are weakened according to the rules specified for the strength (Tang and Hudson 2010).

3.2 Modelling of Worm Single- and Double-Disc Cutters Penetrating Granite Rock Samples

After validating the 2D RFPA model, it was then used to investigate the following behaviours for the granite rock, as functions of the disc cutter's penetration, considering various amounts of wear to the cutter blade: (i) change in cutting force; (ii) the resulting stress distribution within the rock sample; (iii) the process of crack initiation and expansion.

The 2D RFPA model considered a 152×100 mm (breath by depth) sized granite rock sample. These sample dimensions align with laboratory-scale indentation (e.g., BTS) and cutting tests commonly used in rock mechanics practice, while also ensuring sufficient distance occurs between the disc-cutter blade(s) and the rock sample's edges, thereby minimising artificial stress constraint effects. In mechanised tunnelling, the rock mass surrounding the excavation face is confined on all sides due to in-situ geological stresses, that is, apart from at the free surface (zero lateral confinement stress), where it is able to fracture and material can be displaced under the action of the TBM cutter force. To replicate this confined high-stress environment of deep tunnelling in the numerical model, the granite rock sample was restrained within a steel frame having a high modulus of elasticity. This ensured that the model captured critical phenomena (e.g., the stress concentration occurring ahead of the cutter blade within the rock sample, and lateral force generation), such that the model's cutter force, stress distribution and fracture-pattern predictions are grounded in physical reality, bridging the gap between numerical simulation and field-scale tunnelling.

The same 0.5-mm element size (as adopted for simulation of the BTS test: Sect. 3.1) was adopted for discretising the granite rock sample using a 304×200 mesh (60800 elements). Again, this element size strikes a practical balance of maintaining manageable simulation durations, while enabling detailed resolution of the stress gradients, micro-crack initiation (via Weibull-distributed heterogeneity of $m = 5$) and crack dynamics, as validated through mesh convergence studies. The same input properties reported in Sect. 3.1 for the BTS model were adopted here for simulating the granite rock sample and the steel material of the disc cutters, again applying an external vertical displacement rate of 0.005 mm/step to the disc cutter. As presented in Fig. 6, the modelling considered two scenarios: (i) a single-disc cutter positioned

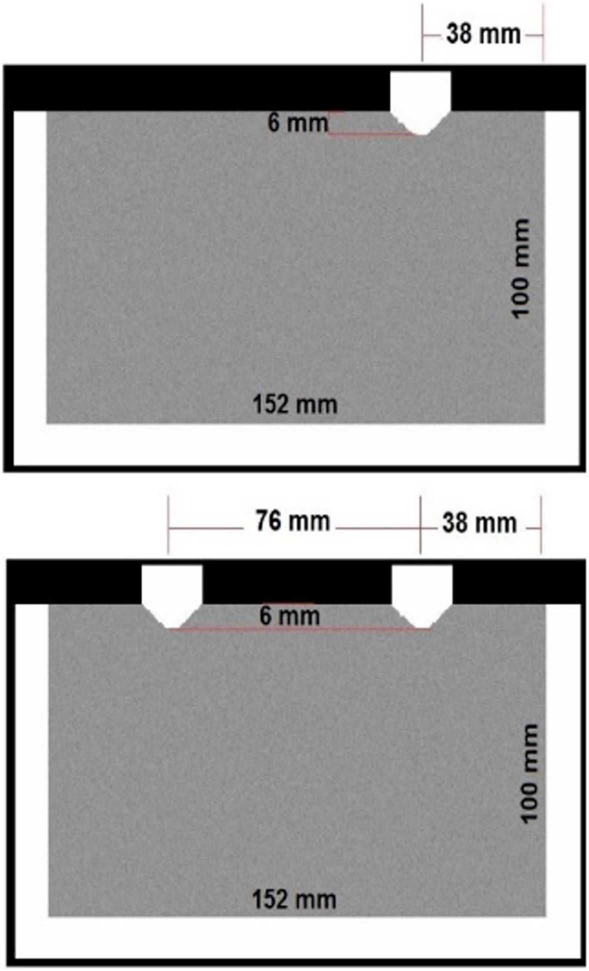

Fig. 6 Geometries of 2D RFPA models for investigating the granite rock fragmentation process using: (**a**) single-disc cutter; (**b**) double-disc cutter. Note: the disc cutters are indicated for a 6-mm penetration depth below the free surface of the laterally restrained rock samples

at a distance of 38 mm from the lateral boundary; (ii) a double-disc cutter, each blade positioned 38 mm from the nearest lateral boundary and with a separation distance of 76 mm between blades. The effect of six levels of wear (i.e., $w=0$, 4, 8, 12, 16 and 20 mm) to the cutter blade were investigated for both scenarios.

4 Numerical Results

4.1 Validation of Numerical Model against BTS Results

Figure 7 presents typical simulation results obtained for the 20th, 30th and 42nd load steps of the BTS test on the granite rock core. Figure 7(a) shows the distribution of damaged elements in the BTS core for each of these load steps. In Fig. 7(b), the brightness indicates the maximum shear stress distribution, while Fig. 7(c) presents the tensile failure progression across the core's diameter (i.e., for the diametrical

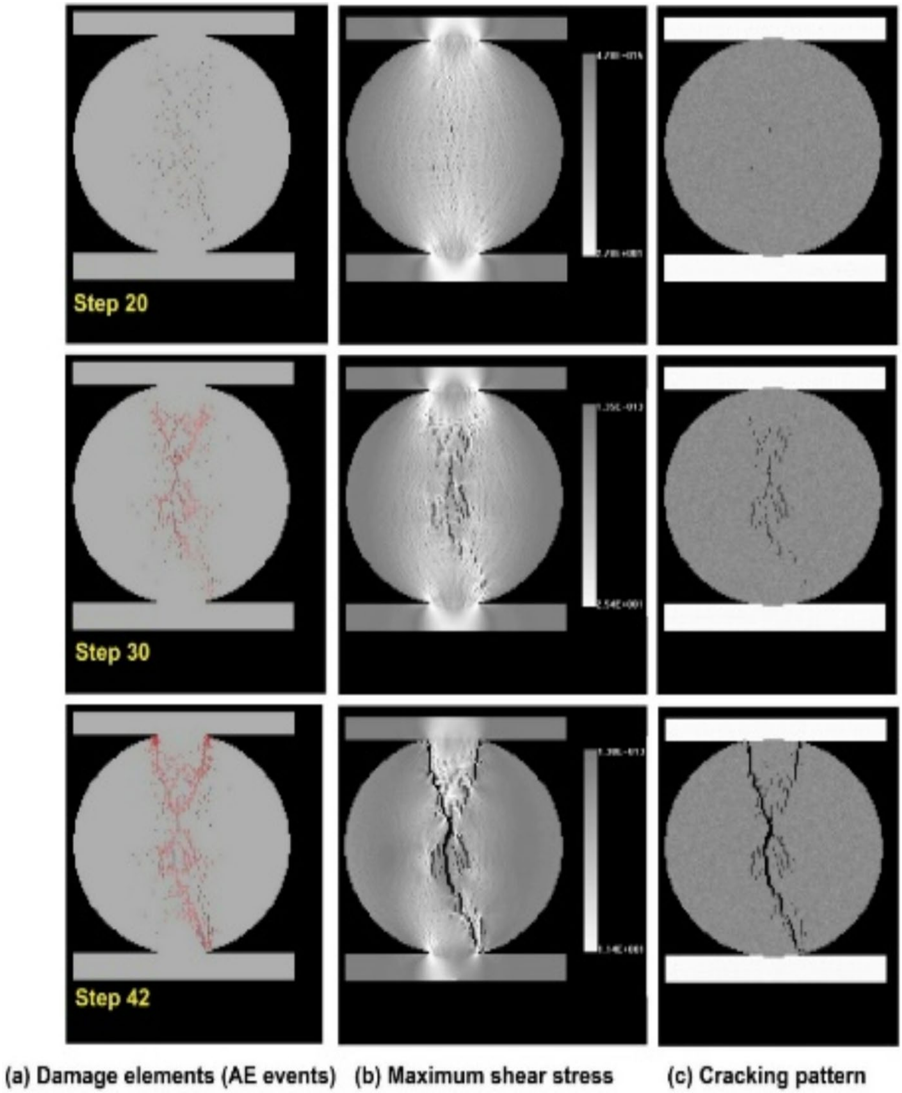

Fig. 7 Fracture progression in granite rock core predicted by 2D RFPA model for BTS test: (**a**) distribution of damaged elements; (**b**) maximum shear stress; (**c**) cracking pattern. Note: in the online version of Fig. 7(a), the red and blue colours indicate those elements damaged (in shear and tension, respectively) at the current load step, whereas the black coloured elements experienced damage during earlier load steps

loading condition of the BTS test). In other words, micro-cracks form due to tensile/shear stresses exceeding the rock's strength, crack growth occurring in the direction of maximum (major) principal stress (σ_1), with adjacent cracks linking up (coalescence) to create a continuous failure surface.

Figure 8 shows the platen load–displacement curve from the simulation, which predicted a maximum (failure) load of $P = 643$ N. Accordingly, the tensile strength

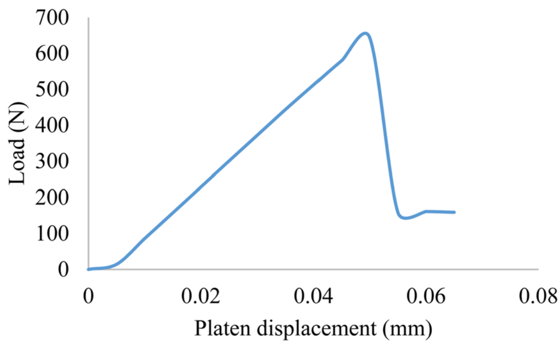

Fig. 8 Platen load–displacement curve predicted by the 2D RFPA model for the 54-mm dia. granite rock core in the BTS test

from the model is computed using Eq. 2 as $\sigma_t = 7.6$ MPa (i.e., in excellent agreement with the experimental mean BTS value of $\sigma_t = 7.7$ MPa, indicating the reliability of the simulation results).

$$\sigma_{\mathrm{t}} = \frac{2P}{\pi\ t\ D} \tag{2}$$

where σ_t is the BTS (in MPa), P is the maximum load (in Newtons), with D and t being the rock core's diameter and length/thickness, respectively (both given in millimetres).

Comparing the model predictions against the BTS results, the simulated platen load–displacement curve closely matched the experimental trend, adequately capturing both the peak load magnitude and the post-failure behaviour. This quantitative alignment — with a BTS deviation of less than 16% — demonstrated the model's ability to accurately simulate the deformation and brittle fracture mechanics inherent to granite rock under tensile loading. Qualitatively, the model's predicted fracture pattern mirrored the laboratory observations, i.e., along the vertical diameter of the BTS rock core, the simulation reproduced the sequence of crack initiation, followed by coalescence and finally core splitting. The radial tensile cracks and their propagation paths matched the experimental fracture morphology, confirming that the model realistically captured the crack dynamics and stress redistribution. These validations, which provided the authors with high confidence in the model's accuracy, established a reliable basis for performing subsequent simulations investigating the effects of disc-cutter wear, ensuring that the stress distributions, energy consumption metrics and crack propagation trends derived from the model are grounded in physically realistic mechanics.

4.2 Results for Worm Single- and Double-Disc Cutters Penetrating Granite Rock

4.2.1 Rock Fragmentation Process

Figures 9 and 10 illustrate the rock fragmentation process for the indentation tests, modelling the effect of the worn single- and double-disc cutters (case presented is for $w = 8$ mm) in terms of (a) the distribution of damaged elements, (b) the maximum

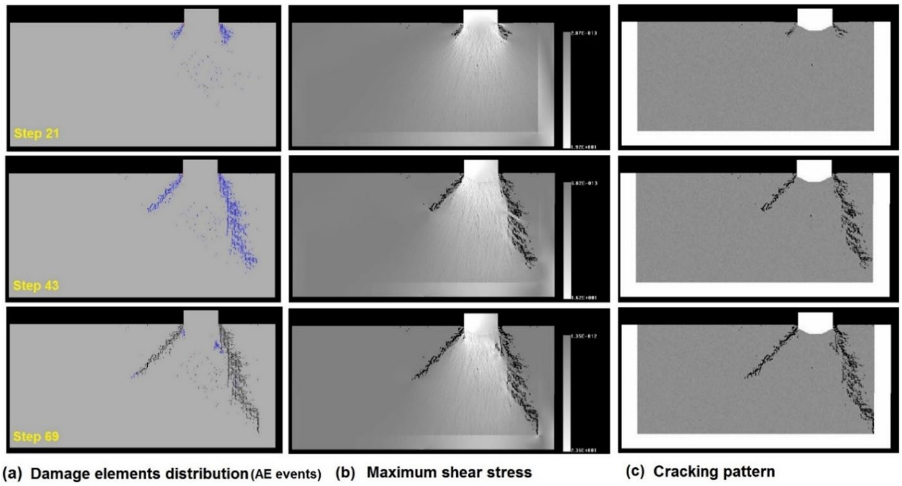

Fig. 9 Numerical simulation of fragmentation process for granite rock sample caused by step penetration of worn single-disc cutter (w=8 mm): (**a**) distribution of damaged elements; (**b**) maximum shear stress; (**c**) cracking pattern. Note: the blue coloured elements evident in the online version of Fig. 9(a) indicate those elements damaged in tensile failure at the current loading step, whereas the black coloured elements experienced damage during earlier load steps

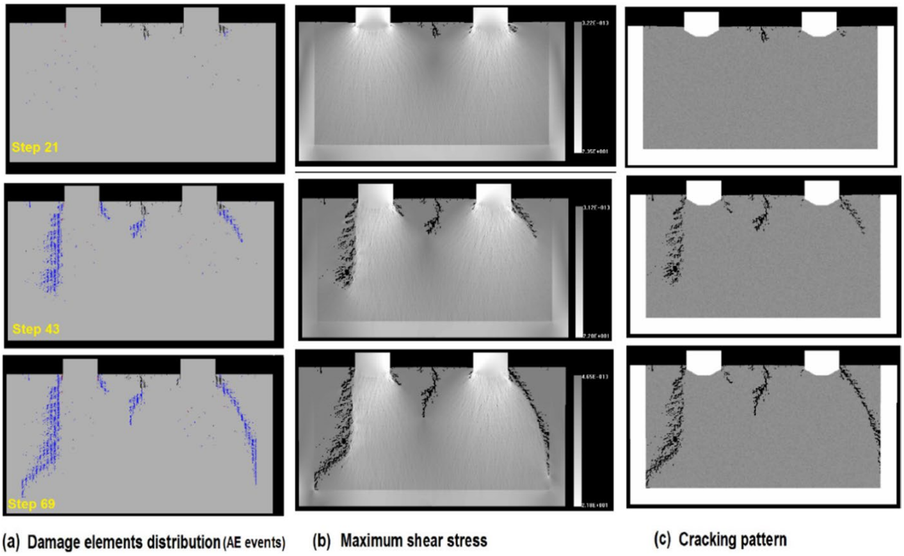

Fig. 10 Numerical simulation of fragmentation process for granite rock sample caused by step penetration of worn double-disc cutter (w=8 mm): (**a**) distribution of damaged elements; (**b**) maximum shear stress; (**c**) cracking pattern. Note: the blue coloured elements evident in the online version of Fig. 10(a) indicates those elements damaged in tensile failure at the current loading step, whereas the black coloured elements experienced damage during earlier load steps

shear stress and (c) the cracking pattern. Referring first to the predictions for the worn single-disc cutter shown in Fig. 9; crack initiation occurred at load step 21, as evidenced by the presence of a series of micro-cracks that formed in response to the increase in tensile stress (blue coloured elements) caused by the 0.105-mm penetration of the granite rock sample by the cutter blade. With increasing indentation, the micro-cracks in the rock sample grow and merge into a dominant fracture network, with the propagation of fractures mainly occurring on the right-hand side of the cutter blade's location (i.e., propagating towards the right-side sample boundary). In step 69 (i.e., for 0.345-mm penetration depth), a rock chip has formed to the right-hand side of the single-disc cutter, whereas to its left-hand side, the crack growth (fracture) still remains within the rock sample on account of the larger distance of the cutter blade from the left-side boundary.

For the model investigating the worn double-disc cutter (Fig. 10), the rock fragmentation process was similar to that produced for the single-disc cutter, although the cracks that formed between the two blades of the double-disc cutter were interconnected (because of their close proximity to one another), resulting in rock chips developing to both the right- and left-hand sides of the rock sample.

The modelling results for single- and double-disc cutters with other amounts of wear (i.e., for $w=0$, 4, 12, 16 and 20 mm) revealed almost identical fragmentation of the rock samples to those shown for $w=8$ mm in Figs. 9 and 10.

4.2.2 Indentation Force–Depth Relationship Considering Different Amounts of Wear to the Cutter Blade

Figure 11 shows the numerically predicted indentation force–depth plots for the single- and double-disc cutters penetrating into the granite rock sample, considering all six wear cases of $w=0$, 4, 8, 12, 16 and 20 mm. The overall trend evident in this figure indicates that the peak indentation force increases for greater amounts of wear to the cutter blade. Another important observation concerns the shape (extent) of the indentation force–depth plots. In other words, less worn cutters produced more compact plots, indicative of brittle-type rock failure. Whereas, increasing wear of the cutter blades produced more open plots, indicative of more ductile-type behaviour.

Figure 12 shows the peak indentation force predicted for different amounts of wear to the cutter blade. As expected, an overall increase in the peak indentation force occurs for increasing wear, which is simply explained by the reduced magnitude of the contact stresses mobilised ahead of the cutter blade (i.e., on account of the increased cutter blade–rock contact area for a given indentation depth). Note the significant increases in peak indentation force required for single- and double-blade cutter discs with more than 8 and 12 mm of wear, respectively.

Additionally, closer examination of the plots in Fig. 12 reveals fluctuations in the peak indentation force magnitudes (decrease, increase and eventual decrease) with increasing wear of the blades, i.e., from $w=8$ to 20 mm. These fluctuations are attributed to the interplay between the residual rock strength, stress redistribution and evolving failure mechanisms, with their occurrence explained as follows. At lower wear levels ($w \leq 8$ mm), the cutter blade retains sufficient sharpness, generating localised stress concentrations in the intact rock sample that induce brittle-type

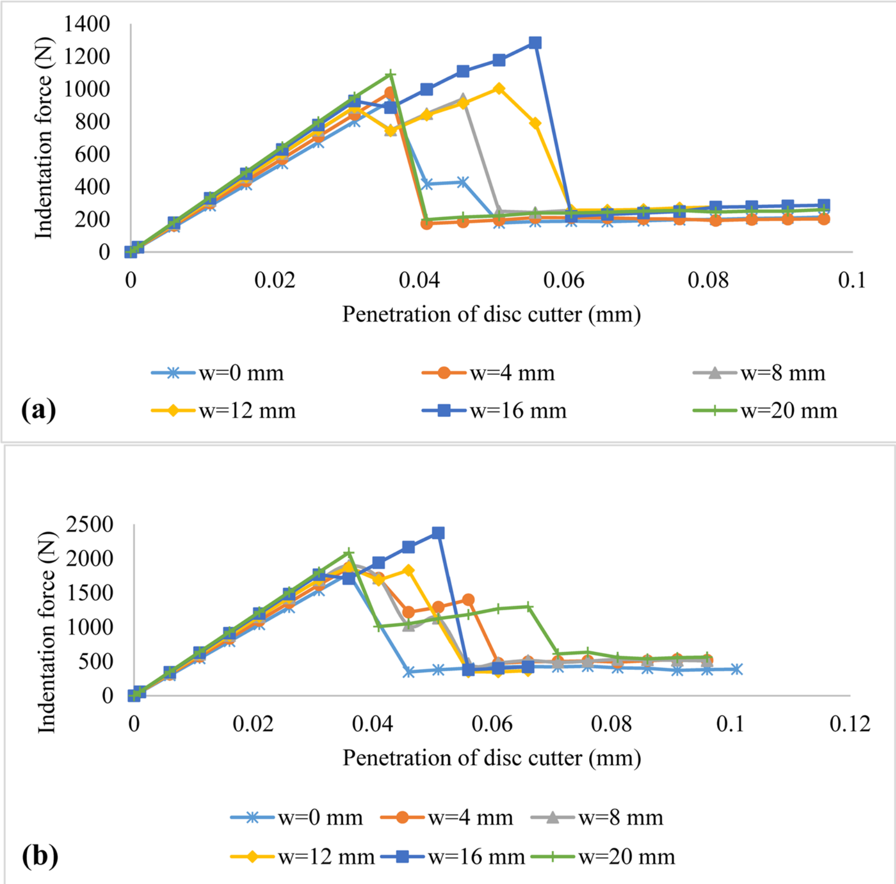

Fig. 11 Numerical indentation force–depth plots predicted for cutter blades with different amounts of wear when penetrating into a granite rock sample: (**a**) single-disc cutter; (**b**) double-disc cutter

fracture (rapid crack initiation and chip formation). As the amount of wear increases from $w = 12$ to 16 mm, the blunted cutter blade distributes the indentation stress over a wider contact area with the rock sample, causing the failure mode to change from brittle-type fracture to a more ductile-type response, i.e., the rock sample undergoes some additional plastic deformation rather than clean chipping. The residual strength of the crushed rock zone now acts as a "secondary load-bearing" layer. To overcome its resistance, the blunted cutter blade must exert additional indentation force to further pulverise the rock material, i.e., resulting in a slight increase in the required peak indentation force. Whereas for severe wear cases (of $w = 16$–20 mm), under the action of the applied indentation force, the rock material ahead of the blunt cutter blade is fully pulverised into a fine-grained debris layer. This eliminates its residual strength, explaining the drop off in peak indentation force for increasing w from 16 to 20 mm, since the advancing cutter blade merely displaces this pulverised rock material (rather than having to fracture intact rock).

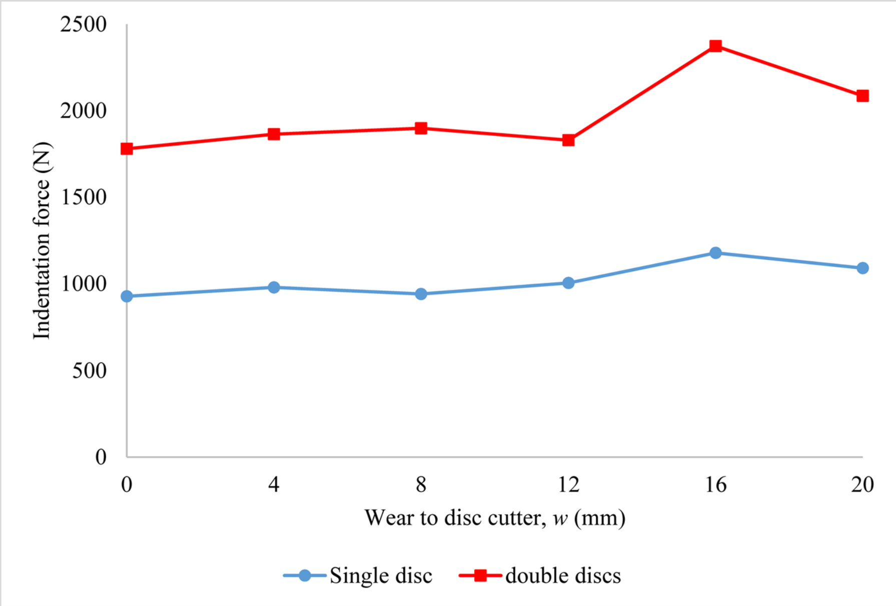

Fig. 12 Predicted variations in the peak indentation force for the granite rock sample with respect to the amount of wear to the cutter blades

4.2.3 Energy Consumption for Crack Propagation Considering Different Amounts of Wear to the Cutter Blade

The energy consumption (W) necessary for crack propagation is an important parameter affected by the amount of disc cutter wear. Figure 13 presents the predicted variation in W (computed according to Eq. 2) with respect to the amount of blade wear, as the cutter penetrates into the granite rock sample. Similar to the earlier observations regarding the peak indentation force, this figure predicts that the energy consumption increases overall for greater amounts of wear to the cutter blade, i.e., rock excavation by TBMs becomes more energy intensive for greater cutter-blade wear.

$$W \approx \sum_{i=1}^{n} F_i \triangle u_i \tag{3}$$

where F_i and u_i are the indentation force and depth magnitudes predicted for the ith step, respectively.

4.2.4 Stress Distribution Within the Rock Sample Considering Different Amounts of Wear to the Cutter Blade

Figure 14 presents the predicted distributions of the major principal stress (σ_1), minor principal stress (σ_3) and shear stress (τ) acting in the width of the rock sample (for the 2D plane-strain model) considering sharp single- and double-disc cutters (i.e., w=0 mm). The selection of these particular stresses for analyses is rooted in their

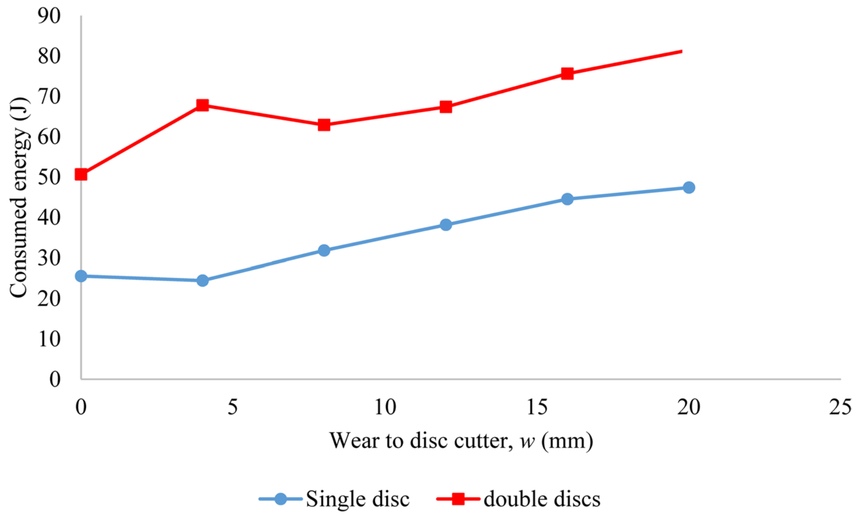

Fig. 13 Predicted variations in energy consumption necessary for crack propagation in granite rock sample considering different amounts of wear to the cutter blades

fundamental roles in rock mechanics, and their direct relevance to cutter–rock interaction dynamics. In other words, when σ_1 exceeds the rock's tensile strength, tensile cracking initiates — a dominant fragmentation mechanism for brittle rock material. Whereas σ_3 represents the lateral confinement stress, which inhibits crack propagation by increasing the shear strength of the rock (in line with the Mohr–Coulomb criterion). This is critical for understanding how the stress redistribution occurring within the rock sample under the increasing indentation forces changes with the amount of cutter wear. While the shear stress (τ) drives slip along planes of weakness; a key mechanism in the more ductile-type failure response observed for worn cutters — with this shear-dominated failure consuming more energy and delaying chip formation. Additionally, in revealing tensile crack initiation zones, σ_1 serves as a guide in cutter-head design to optimize chip formation. In highlighting confinement effects, σ_3 informs decisions on the spacing of the disc cutters located in the TBM cutter-head, as well as the thrust force adjustments. While the shear stress magnitude correlates with energy dissipation in grinding-dominated rock failure, explaining the efficiency losses for worn disc cutters. Note: the x-axes of the plots presented in Fig. 14 are zoomed-in views of specific regions of interest where the stress concentrations occur — specifically, the areas in front of and between the disc cutter blades.

Referring to Fig. 14; across the breath of the rock sample, the values of the σ_1, σ_3 and τ stresses increase steeply in front of the sharp cutter blades, with Fig. 14(a) presenting one set of stress peaks mobilised for the single-disc cutter, while two sets of stress peaks occur in Fig. 14(b) for the double-disc cutter. In terms of magnitude, the shear stress falls between σ_1 and σ_3.

Figures 15 and 16 show the effect of cutter wear (i.e., considering the cases of $w = 0$, 12 and 20 mm) on the σ_1 distribution within the rock sample for single- and double-disc cutters, respectively. Note that in the online version of this figure, the peak σ_1 range for each case is indicated by red dashed-line boundaries.

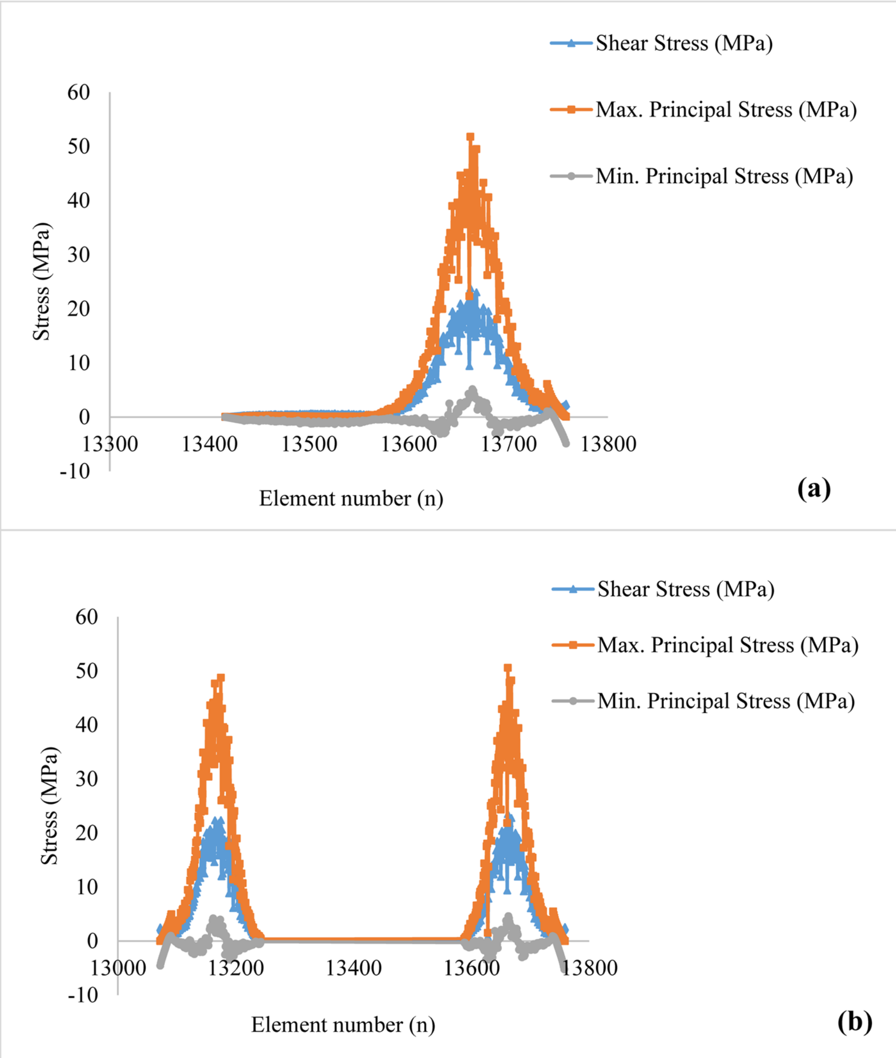

Fig. 14 Predicted distributions of the major principal stress, minor principal stress and shear stress mobilised within the granite rock sample for sharp disc cutters: (**a**) single-disc cutter; (**b**) double-disc cutter. Note: for the x-axis, the global element numbering is used, each element being 0.5-mm in size

For a sharp single-disc cutter (Fig. 15(a)), the peak σ_1 value of ~51.8 MPa occurs directly ahead of the cutter blade, with the stress magnitude gradually reducing for moving away from the disc's vertical axis, reaching a zero σ_1 value in the border elements. However, as shown in Figs. 15(b, c), the trends are significantly different in the case of the blunted cutter blade (i.e., for $w = 12$ and 20 mm). Here, the σ_1 stress growth is quite sharp, with the peak σ_1 mobilised over a significant width of the sample face. Considering the number of elements (each 0.5-mm sized for the model) between the dashed-line boundaries in these figures, the predicted widths of the peak

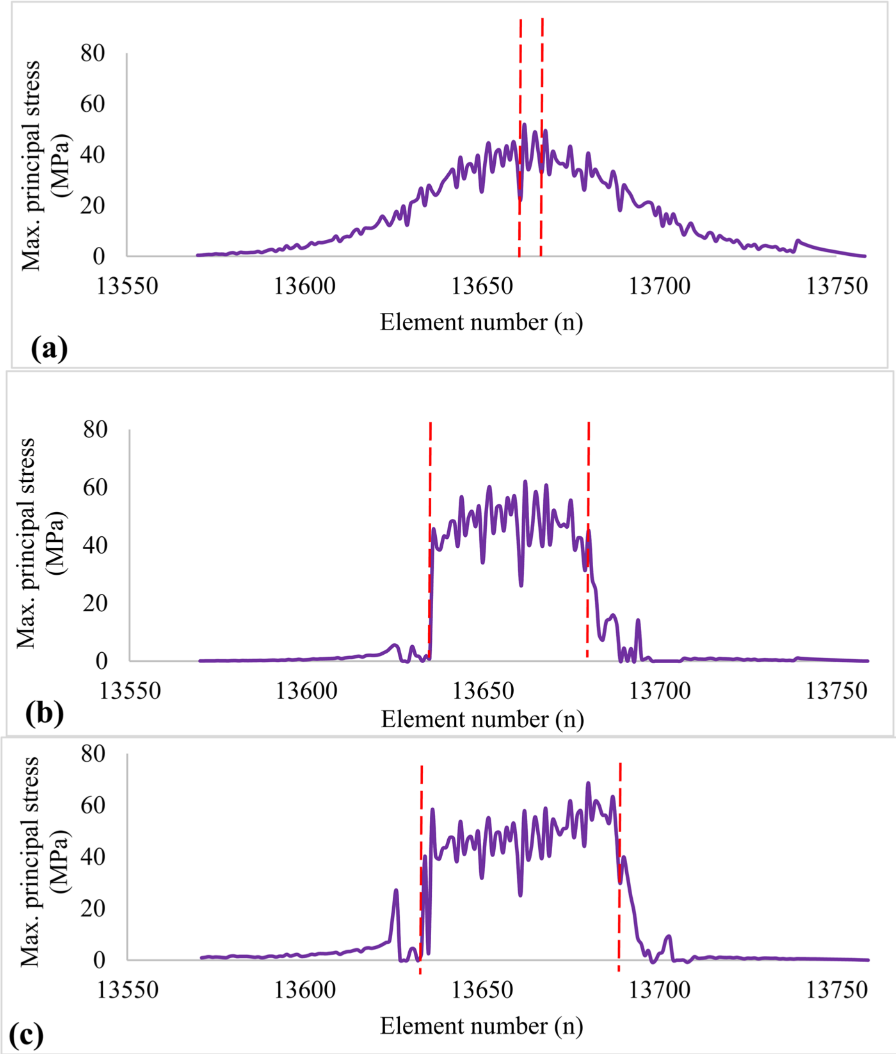

Fig. 15 Major principal stress distribution for single-disc cutter, considering the cases of (**a**) $w = 0$ mm, (**b**) $w = 12$ mm and (**c**) $w = 20$ mm

σ_1 range for single-disc cutters with wear levels of $w = 0$, 12 and 20 mm were computed as approximately 3.0, 19.5 and 28.0 mm, respectively.

Similar to the single-disc cutter; according to Fig. 16(a), the peak σ_1 values of ~50.6 MPa for a sharp double-disc cutter occurred directly ahead of the cutter blades, with the stress magnitudes gradually decreasing, reaching a zero σ_1 value in the border elements. Furthermore, as shown in Figs. 16(b, c) for the worn disc cutters (i.e., $w = 12$ and 20 mm), the σ_1 stress growth is also quite sharp, with two peak σ_1's occurring over significant widths ahead of the blunted blades. Using the same approach described above, the predicted widths of the peak σ_1 range for double-disc cutters

Fig. 16 Major principal stress distribution for double-disc cutter, considering the cases of (**a**) $w = 0$ mm, (**b**) $w = 12$ mm and (**c**) $w = 20$ mm

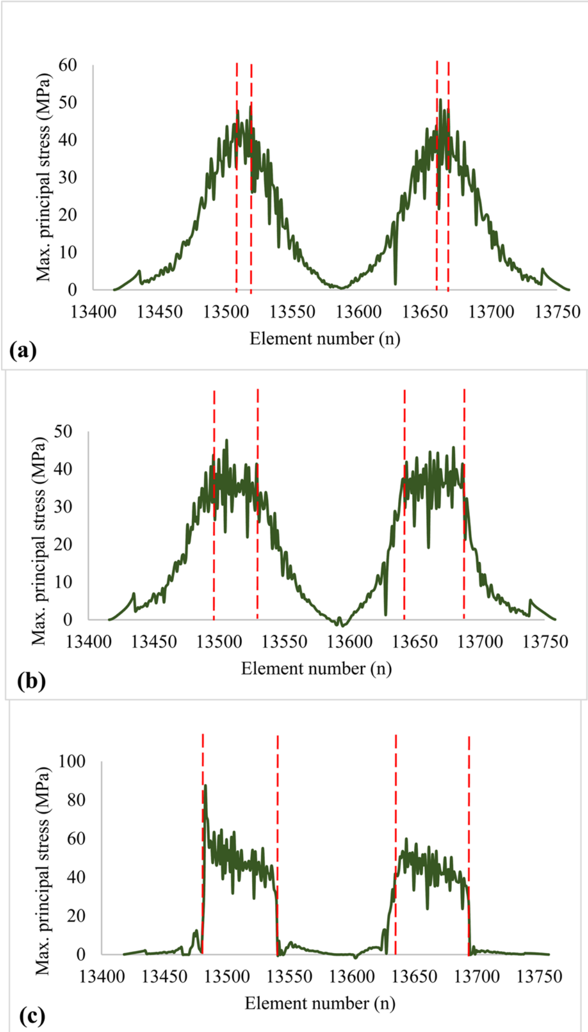

with $w = 0$, 12 and 20 mm were computed as approximately 5.0, 16.0 and 26.5 mm, respectively.

5 Discussion

This numerical investigation advances TBM cutter management by challenging simplifications adopted in earlier research studies that treated rock as homogeneous (e.g. Xu et al. 2021) or cutter wear as binary (e.g. Wu et al. 2019), and which focused on the effect of the confinement stress (Ma et al. 2011) or assumed idealised tool–rock interactions (Huang et al. 2013). Whereas the models employed in the present investigation integrated granular cutter-wear analysis (for w in the range of 0 to 20 mm) with Weibull-distributed rock heterogeneity to quantify how progressive wear of the cutter blades alters the failure mode for the granite rock material encountered in the KSWCT project. The results revealed nonlinear trends in the indentation force and energy consumption for increasing wear of the single- and double-disc cutter types. Compared to the single-disc cutter, double-disc cutters (with 76-mm spacing between them) reduce the SE of excavation by some 15–20% via inter-disc crack interactions, thereby shifting the design paradigms from quantity to strategic placement of the cutters over the TBM cutter-head. Sharp cutter blades were found to generate concentrated localised stresses in the intact rock, promoting rapid crack initiation and coalescence (brittle fracture) for the granite rock, whereas the indentation force–depth curves for worn cutter blades exhibited a more ductile-type behaviour, which required significantly higher peak indentation force to induce fracture. This divergence in behaviour arises from the altered interaction dynamics between the cutter blade and granite rock material under varying wear levels. In other words, when the sharp concentrated stress distribution generated in front of the new cutter blades surpasses the yield strength, the rock matrix fractures with minimal energy expenditure. Conversely, worn cutter blades generate diffuse and dispersed stress fields due to blunted geometries and reduced contact efficiency. This dispersion redistributes stress over a wider area, delaying the accumulation of the critical stress levels required for chip formation. Consequently, the rock cutting process becomes less efficient, necessitating prolonged mechanical engagement to achieve the same indentation depth — a key finding of the present case-study being that cutter wear must be limited to 8–12 mm to avoid energy penalties during TBM excavation in the KSWCT granite rock. Moreover, the presented energy–wear relationship (in Fig. 13) extends beyond traditional force-based analyses, providing actionable data for optimising cutter replacement schedules. For instance, in the KSWCT project, the energy consumption of TBM excavation significantly increased for more than 12-mm of wear to the cutter blades, correlating with 25–30% declines in the tunnelling advance rates. In other words, the interplay between the blade wear, stress distribution and fracture mechanics directly dictates the TBM's excavation performance, with a progressive decline in the drilling efficiency occurring as the cutter wear intensifies, leading to higher TBM torque demands, elevated wear rates for adjacent mechanical components and extended cycle times. This 12-mm wear threshold applied to the cutter blades, established for the KSWCT granite rock in the present investigation, advocates a paradigm shift in maintenance strategies, i.e., mandating threshold-based maintenance over generic reactive "replace-when-worn" maintenance guidelines. This threshold based cutter-wear maintenance approach contrasts with existing approaches prioritising cutter spacing (Moon and Oh 2012) or lateral forces, i.e., which do not consider cutter wear–energy consumption correlations (Sabri et al. 2023). Furthermore, the delayed fracture mechanics associated with worn cutter blades exacerbate tool vibration and produce irregular cutting patterns, increasing the risk of premature tool failure or damage caused to the TBM's cutter-head structure.

Of course, the ideal operational scenario would involve maintaining the cutter blades in a near-intact state to leverage their brittle fracture mode advantage over that produced by blunted cutter blades. The main strategies for minimising the cutter wear in hard rock excavation include: (i) employing cutters manufactured using advanced wear-resistant alloys or coatings, particularly for the central and radius cutters located in the cutter-head; (ii) optimising the cutter spacing and penetration depth to reduce contact stresses and abrasion; (iii) reducing the TBM thrust force or adjusting tunnelling advance rates in highly abrasive zones to prolong the cutter life; (iv) adopting real-time wear monitoring, e.g., employing IoT-enabled sensor-equipped TBM cutter-heads, to track the cutters' health and trigger cutter replacements before adverse wear-induced efficiency losses occur. Proactive inspection intervals — calibrated to real-time wear monitoring systems — are essential to pre-emptively identify and replace degraded cutters before they compromise operational efficiency, i.e., optimising the cutter replacement schedules not only mitigates downtime, but also reduces long-term operational costs by aligning maintenance activities with predictive wear models. By prioritising sharp, intact cutters, the TBM plant can sustain the efficient brittle fracture mode, thereby minimising energy consumption, maximising advance rates and reducing project costs in large-scale tunnelling operations.

It should be mentioned that while the 2D RFPA models employed in the present investigation capture planar fracture mechanics, balancing computational efficiency with sufficient accuracy, nevertheless they neglect the 3D stress concentrations or torsional effects inherent in the rotating TBM cutter-head — a gap addressable via, for instance, coupled DEM–FEM frameworks. Additionally, the model validation is limited to Brazilian tensile strength tests, which may not adequately represent the complex stress conditions encountered during actual TBM operation. As such, the numerical simulations would benefit from more comprehensive experimental validation and comparison with field performance data. Furthermore, while the 12-mm cutter wear threshold recommendation applies for TBM excavation in the KSWCT granite rock, further research evidence is need to support its broad applicability across diverse rock types, geological conditions or TBM configurations/operating conditions.

6 Summary and Conclusions

Through granular wear analysis (for $w = 0$–20 mm) and Weibull-distributed heterogeneity modelling, the present case study employed numerical modelling to investigate the effect of TBM disc-cutter wear on the rock fragmentation efficiency for granite rock sourced from the KSWCT project (Iran), with the following conclusions:

- Compared to sharp disc cutters that produce brittle fracture of the KSWCT granite rock, progressive wear of the cutter blade increases the peak indentation (cutting) force by 20–40%, with blunted cutters also producing a more ductile-type rock failure mode.
- As the disc cutter wears, the energy consumption necessary for crack propagation substantially increases, i.e., the rock cutting process becomes more energy intensive.
- Disc-cutter wear affects the stress distribution profile in the intact granite rock; a sharp concentrated stress profile being observed ahead of new disc cutters, whereas the stress concentration occurred over a wider band for blunted cutters.
- The identification of a critical 12 mm cutter-wear threshold for the KSWCT gran-

ite rock — beyond which the energy consumption increased by 35% — provides a data-driven basis for predictive maintenance of the TBM's disc cutters.

Furthermore, integrating stochastic rock behaviour, granular wear analytics and field-derived thresholds establishes a scalable blueprint for optimising cutter life and tunnelling efficiency in abrasive rock environments. These insights not only refine existing models and maintenance strategies, but also propel data-driven TBM practices into a new era of sustainability and cost-effectiveness for global hard-rock excavation projects.

Some key recommendations include prioritising the replacement of worn central and radius cutters, optimising cutter spacing and deploying IoT-enabled monitoring to pre-empt tunnelling efficiency losses. These strategies, validated against field data from the KSWCT project, reduced downtime by 20–30% as well as operational costs by 15–25%, thereby offering a paradigm shift from trial-and-error practices to precision engineering.

By bridging stochastic mesoscale modelling with macroscale TBM performance, this work not only advances academic understanding of wear-driven fracture mechanics, but also delivers actionable protocols for sustainable tunnelling in abrasive rock environments. Future research work should expand the presented 2D models into 3D stress modelling, as well as cross-lithology validation, to universalise these insights, ensuring their global applicability. Ultimately, by contextualising wear-driven inefficiencies within micromechanical and operational frameworks, this case-study redefines TBM cutter management as a synergy of predictive analytics and geomechanical innovation, setting a new standard for efficiency and cost-effectiveness in mechanised tunnelling.

Author Contributions Mansour Sabri: conceptualisation, methodology, software, formal analysis, resources, data curation, writing—original draft. Ebrahim Sharifi Teshnizi: methodology, formal analysis, investigation, data curation, writing—original draft, supervision, writing—review and editing. Kamran Goshtasbi: conceptualisation, investigation, writing—original draft, supervision. Hamid Reza Nejati: investigation, resources, writing—original draft. Ehsan Taheri: investigation, resources, writing—original draft. Brendan C. O'Kelly: writing—review & editing. All authors reviewed the manuscript.

Funding Open Access funding provided by the IReL Consortium. This research did not receive any specific grant from funding agencies in the public, commercial, or not-for-profit sectors.

Data Availability Data that support the findings of this study are available from the corresponding author upon reasonable request.

Declarations

Competing interests The authors declare no competing interests.

References

Chen, L.H., Labuz, J.F.: Indentation of rock by wedge-shaped tools. International Journal of Rock Mechanics and Mining Sciences **43**(7), 1023–1033 (2006). https://doi.org/10.1016/j.ijrmms.2006.03.005

Chen, Y., Song, C.: Rock fragmentation characteristics by TBM cutting and efficiency under bi-lateral confinement. Applied Sciences **8**(4), 498 (2018). https://doi.org/10.3390/app8040498

Huang, H., Lecampion, B., Detournay, E.: Discrete element modeling of tool-rock interaction I: Rock cutting. International Journal for Numerical and Analytical Methods in Geomechanics **37**(13), 1913–1929 (2013). https://doi.org/10.1002/nag.2113

Lin, Q.B., Cao, P., Li, K.H., Cao, R.H., Zhou, K.P., Deng, H.W.: Experimental study on acoustic emission characteristics of jointed rock mass by double disc cutter. Journal of Central South University **25**(2), 357–367 (2018). https://doi.org/10.1007/s11771-018-3742-7

Liu, J., Cao, P., Han, D.: Sequential indentation tests to investigate the influence of confining stress on rock breakage by tunnel boring machine cutter in a biaxial state. Rock Mechanics and Rock Engineering **49**(4), 1479–1495 (2016). https://doi.org/10.1007/s00603-015-0843-6

Ma, H., Yin, L., Ji, H.: Numerical study of the effect of confining stress on rock fragmentation by TBM cutters. International Journal of Rock Mechanics and Mining Science **48**(6), 1021–1033 (2011). https://doi.org/10.1016/j.ijrmms.2011.05.002

Moon, T., Oh, J.: A study of optimal rock-cutting conditions for hard rock TBM using the discrete element method. Rock Mechanics and Rock Engineering **45**(5), 837–849 (2012). https://doi.org/10.1007/s00603-011-0180-3

Sabri, M., Goshtasbi, K., Nejati, H.R., Taheri, E.: A numerical investigation of the effect of disc cutter wear on rock-cutting forces in mechanized tunnel boring machines. International Journal of Geomechanics **23**(5), 04023050 (2023). https://doi.org/10.1061/IJGNAI.GMENG-8006

Sabri, M., Goshtasbi, K., Reza Nejati, H., Taheri, E.: Evaluation of the effect of TBM disc cutter wear on rock cutting efficiency. Geomech. Tunn. **17**(2), 146–156 (2024). https://doi.org/10.1002/geot.202300015

Tang, C., Hudson, J.A.: Rock Failure Mechanisms. CRC Press/Balkema. (2010). https://doi.org/10.1201/b10997

Tang, C., Tang, S.: Applications of rock failure process analysis (RFPA) method. Journal of Rock Mechanics and Geotechnical Engineering **3**(4), 352–372 (2011). https://doi.org/10.3724/SP.J.1235.2011.00352

Tang, C., Tang, S.: Applications of rock failure process analysis (RFPA) to rock engineering. In: Shen, B., Stephansson, O., Rinne, M. (eds.) Modelling Rock Fracturing Processes. Springer, Cham (2020). https://doi.org/10.1007/978-3-030-35525-8_17

Wang, S.Y., Sloan, S.W., Liu, H.Y., Tang, C.A.: Numerical simulation of the rock fragmentation process induced by two drill bits subjected to static and dynamic (impact) loading. Rock Mechanics and Rock Engineering **44**(3), 317–332 (2011). https://doi.org/10.1007/s00603-010-0123-4

Wang, Z., Cao, P., Chen, Y.: Study on the optimum penetration depth by two TBM cutters under different cutter spacings. Journal of Vibroengineerin**21**(4), 864–875 (2019). https://doi.org/10.21595/jve.2018.20079

Wu, Z., Zhang, P., Fan, L., Liu, Q.: Numerical study of the effect of confining pressure on the rock breakage efficiency and fragment size distribution of a TBM cutter using a coupled FEM-DEM method. Tunnelling and Underground Space Technology **88**, 260–275 (2019). https://doi.org/10.1016/j.tust.2019.03.012

Xu, H., Geng, Q., Sun, Z., Qi, Z.: Full-scale granite cutting experiments using tunnel boring machine disc cutters at different free-face conditions. Tunnelling and Underground Space Technology **108**, 103719 (2021). https://doi.org/10.1016/j.tust.2020.103719

Zhu, W.C., Tang, C.A.: Micromechanical model for simulating the fracture process of rock. Rock Mechanics and Rock Engineering **37**(1), 25–56 (2004). https://doi.org/10.1007/s00603-003-0014-z

Zhu, W.C., Tang, C.A.: Numerical simulation of Brazilian disk rock failure under static and dynamic loading. International Journal of Rock Mechanics and Mining Sciences **43**(2), 236–252 (2006). https://doi.org/10.1016/j.ijrmms.2005.06.008

Authors and Affiliations

Mansour Sabri[1] · Ebrahim Sharifi Teshnizi[2] · Kamran Goshtasbi[1] · Hamid Reza Nejati[1] · Ehsan Taheri[1] · Brendan C. O'Kelly[3]

✉ Brendan C. O'Kelly
bokelly@tcd.ie

Mansour Sabri
m.sabri@modares.ac.ir

Ebrahim Sharifi Teshnizi
Ebrahim.SharifiTeshnizi@mail.um.ac.ir

Kamran Goshtasbi
goshtasb@modares.ac.ir

Hamid Reza Nejati
h.nejati@modares.ac.ir

Ehsan Taheri
e_taheri@modares.ac.ir

[1] Department of Mining Engineering, Tarbiat Modares University, Tehran, Iran

[2] Department of Geology, Ferdowsi University of Mashhad, Mashhad, Iran

[3] Department of Civil, Structural and Environmental Engineering, Trinity College Dublin, Dublin, Ireland